IBIMA Publishing
Communications of International Proceedings
https://ibimapublishing.com/p-articles/46ICT/2025/4639925/
Vol. 2025 (35), Article ID 4639925

Multi-Sensor Fusion for Indoor Positioning System*

Mateusz DWORACZYK[1], Maria ROSIAK[1], Mateusz KAWULOK[1], Stella MAĆKOWSKA[2]
And Michał MAĆKOWSKI[1]

[1]Department of Distributed Systems and Informatic Devices, Faculty of Automatic Control, Electronics and Computer Science, Silesian University of Technology, Akademicka 16, 44-100 Gliwice, Poland

[2]Department of Medical Informatics and Artificial Intelligence Faculty of Biomedical Engineering, Silesian University of Technology, Roosevelta 40, 41-800 Zabrze, Poland

Correspondence should be addressed to: Mateusz DWORACZYK, matedwo224@student.polsl.pl

* Presented at the 46th IBIMA International Conference, 26-27 November 2025, Ronda, Spain

Abstract

Diverse sources of radio signal interference and the complex topology of multi-level indoor structures often impede reliable position tracking. Therefore, a solution based on a Pedestrian Dead-Reckoning (PDR) navigation module utilizing high-frequency data from Inertial Measurement Unit (IMU), as well as two complementary technologies: Bluetooth Low Energy (BLE) - employing RSSI-based distance estimation and Ultra-Wideband (UWB), which relies on Time-of-Flight (ToF) signal, was proposed. The continuous, high-frequency motion tracking provided by the IMU was periodically corrected using absolute, though inherently noisy, radio-based measurements. This fusion strategy allowed for the mitigation of drift accumulation, yielding a trajectory estimate that remains both locally smooth over short intervals and globally accurate over extended durations. An Extended Kalman Filter (EKF) served as the fusion mechanism, integrating relative motion estimates from the PDR with absolute positional updates to perform a series of controlled experiments under diverse conditions. The analysis of the collected data revealed that the standalone PDR system exhibited a substantial drift error on average between 10% and 15% of the total traversed distance. Sensor fusion with BLE measurements significantly reduced this error, achieving a localization accuracy of Root Mean Square Error (RMSE) = 0.98 m. Under analogous conditions, the UWB-based system demonstrated a decisive advantage, reaching an accuracy level of RMSE = 0.21 m, corresponding to nearly a fivefold improvement compared to BLE. The experimental results confirm that UWB, when combined with sensor fusion frameworks, provides a balance among positional accuracy and robustness to environmental disturbances, making it effective for precise indoor localization.

Keywords: indoor navigation, sensor fusion, PDR, UWB

Cite this Article as: Mateusz DWORACZYK, Maria ROSIAK, Mateusz KAWULOK, Stella MAĆKOWSKA And Michał MAĆKOWSKI, Vol. 2025 (35) "Multi-Sensor Fusion for Indoor Positioning System " Communications of International Proceedings, Vol. 2025 (35), Article ID 4639925, https://doi.org/10.5171/2025.4639925

Introduction

Indoor environments exhibit high spatial and electromagnetic heterogeneity, encompassing open warehouse spaces as well as intricate corridor networks found in office buildings and hospitals. Global Navigation Satellite System (GNSS) signals undergo significant attenuation when passing through construction materials such as concrete, as well as multiple reflections and distortions called the multipath effect (Ahmad, 2024), which leads to a drastic decrease in positioning accuracy (El-Sheimy and Li, 2021) and causes the signal to become unavailable. Therefore, it is necessary to employ alternative positioning methods (Syazwani et al., 2022).

Two aspects of indoor navigation can be identified. The first is the estimation of the current absolute or relative spatial location of a user or object. The second is leveraging positional information to actively guide the user toward a predefined destination. This process often entails solving a shortest-path problem in a graph representation of the building's structure and can be challenging in dynamic and complex environments.

Radio-based localization technologies, including Wi-Fi, Bluetooth Low Energy (BLE), and Ultra-Wideband (UWB), serve a critical role relative to Inertial Measurement Unit (IMU) sensors by providing absolute or pseudo-absolute positional references within a defined coordinate frame. These references are indispensable for correcting the unbounded drift inherent to Pedestrian Dead-Reckoning (PDR) systems. In contrast to inertial navigation, the positioning error, though potentially substantial, does not accumulate over time, making them ideal sources for periodic corrections in sensor fusion frameworks. Nevertheless, such technologies are vulnerable to indoor-specific phenomena, including multipath interference, signal attenuation by obstacles, sensor noise (e.g., inertial drift) (Jiménez et al., 2009), and Non-Line-of-Sight (NLoS) conditions (Ahmad, 2024), all of which contribute to reduced update frequency, increased noise, and the occurrence of outlier measurements (Yoon et al., 2015).

The indoor environment itself is dynamic and can rapidly alter radio wave propagation characteristics, posing a major challenge for methods relying on radio fingerprinting. An even greater obstacle is posed by magnetic field disturbances. Unlike the relatively homogeneous geomagnetic field observed outdoors, indoor environments exhibit significant magnetic anomalies caused by reinforced concrete, electrical installations, and electronic devices. These localized distortions render the magnetometer, nominally providing an absolute heading reference, unreliable and potentially unusable within many indoor locations (Mur-Artal, Montiel and Tardos, 2015).

Nowadays, UWB technology has the highest achievable precision, capable of centimeter-level accuracy, compared to BLE. This is enabled by the use of ultra-short radio pulses transmitted across a wide frequency spectrum, facilitating highly accurate Time-of-Flight (ToF) or Time Difference of Arrival (TDoA) measurements and exhibiting strong resistance to multipath interference compared to narrowband signals (Ali et al., 2021). In addition, IMU allows continuous trajectory tracking and position estimation solely based on motion data, without requiring communication with any external infrastructure. Modern smartphones integrate compact Micro-Electro-Mechanical Systems (MEMS)-based IMUs, typically composed of accelerometers, gyroscopes, and magnetometers. Accelerometers measure linear acceleration, facilitating the identification of cyclic signal patterns corresponding to human steps, and gyroscopes capture angular velocity, enabling estimation of device orientation and, by extension, user heading. The high-frequency data streams can provide reconstructions of short-term relative displacements and detailed tracking of instantaneous orientation and acceleration changes.

The overall effectiveness of a reliable navigation system is intrinsically linked to its ability to handle both the idiosyncrasies of the indoor environment and the kinematic characteristics of pedestrian motion. Beyond challenges related to motion mapping, two fundamental factors critically affect sensor data quality and must be addressed in system design: pervasive environmental interference and hardware heterogeneity.

This study aims to develop and evaluate an integrated indoor positioning framework that combines inertial and radio-based sensing modalities (such as UWB and BLE) through sensor fusion techniques, in order to enhance localization accuracy, robustness, and continuity in dynamic and heterogeneous indoor environments.

Related Work

Pedestrian motion modeling constitutes one of the most challenging aspects of indoor navigation, as human kinematics are inherently complex. In contrast to rigidly mounted INS in vehicles, a mobile device carried by a pedestrian has an arbitrary and frequently changing orientation (Yeong et al., 2021). Consequently, PDR systems typically decompose the problem into three fundamental stages: step detection, step length estimation, and heading determination.

Step detection, most commonly performed through the analysis of cyclic variations in accelerometer signals, is highly susceptible to errors. Step length estimation is often derived from the amplitude of acceleration (a larger amplitude typically equals a longer step); however, it is strongly dependent on the user's individual characteristics (height or gender), rendering the development of a universal model difficult. The most challenging stage is the estimation of the walking direction, as the orientation of the device often deviates substantially from the user's actual heading. This discrepancy, known as the crab angle (Lin et al., 2024), is typically compensated using nonlinear filtering methods such as the Extended Kalman Filter (EKF), which estimates device orientation in real time.

Applications of indoor localization extend across a broad range of domains, encompassing public facilities (airports, railway stations, and academic campuses), the industrial sector (asset tracking), medicine (patient monitoring (Booranawong et al., 2022), and emergency response operations (Ferreira et al., 2017)). These technologies open up new possibilities for enhancing the accessibility of spaces for individuals with visual impairments (Rosiak, Kawulok and Maćkowski, 2024). As highlighted in (Yapar et al., 2023), the growing demand for precise and dependable navigation systems has accelerated the development of multi-modal, data-integrative localization platforms.

The most effective approach to overcoming the limitations of individual sensing modalities is sensor fusion, defined as the integration of heterogeneous data to achieve a robust estimation (Handbook of Multisensor Data Fusion: Theory and Practice, Second Editi, 2025). This framework enables the combination of relative measurements (from IMUs) with absolute radio-based positioning data (from BLE or Wi-Fi), thereby mitigating measurement uncertainty through the synergistic exploitation of each modality's strengths. Fusion can occur at multiple levels, ranging from raw signal integration to high-level data fusion of processed estimates.

As established by (Zhang et al., 2025) no single sensing modality can provide full reliability in indoor localization. Authors (Zhang et al., 2025) argue that radio technologies such as Wi-Fi and BLE are inherently vulnerable to interference and signal attenuation, whereas IMU suffer from cumulative drift errors necessitating their integration within unified fusion frameworks. A classic example of such integration was demonstrated by (Yoon et al., 2015), where an EKF dynamically mitigated the influence of multipath effects and outliers in BLE data.

More advanced methodologies have been proposed by the authors of the paper (Zhang et al., 2025). Their factor graph optimization approach integrates IMU, UWB, and ultrasonic measurements, automatically adjusting the weighting of each observation. The system achieved a Root Mean Square (RMS) error of 12.3 cm, representing a 38% improvement over conventional EKF-based methods, while maintaining high localization accuracy even with a 40% UWB signal dropout.

An evolutionary step forward was demonstrated by (UPPSATSER.SE: Design of a Method to Improve 5G Indoor Positioning Accuracy Using Sensor Fusion with an IMU and Floor Map Information, 2025), who proposed a fusion framework combining IMU data, 5G positioning, and digital building maps within a particle filter formulation. In this approach, the map serves an active role by rejecting outlier positions (e.g., locations estimated "within walls") and adapting the measurement model to the spatial topology. This method substantially improves positional accuracy relative to the classical EKF, particularly under non-Gaussian error distributions.

In recent years, machine learning (ML)-based fusion methods have gained increasing prominence, combining the interpretability of physical models with the adaptability of neural architectures. Authors (Lauzon, 2017) proposed a

hybrid model merging particle filtering with deep neural networks (DNN), enabling intelligent, noise-resilient motion modeling. The paper (Koutris et al., 2022) employed DNNs to estimate the Angle of Arrival (AoA) of BLE signals using both RSSI and In-phase and Quadrature (IQ) data, achieving 70-cm accuracy and high robustness to environmental dynamics.

The potential of integrating multiple sensory modalities - including inertial and visual data - was further demonstrated by (Poulose and Han, 2019), who fused IMU and smartphone camera inputs within an ORB-SLAM framework augmented by a KF. Their hybrid system achieved an average positional error of 0.1398 m, demonstrating the efficacy of multi-sensor fusion in mitigating the intrinsic limitations of single-modality systems.

Advanced filtering techniques, such as the EKF, Particle Filter, and Rauch–Tung–Striebel (RTS) Smoother (Yoon et al., 2015; Khodarahmi and Maihami, 2023), constitute the computational backbone of contemporary sensor fusion frameworks, ensuring both precision and resilience against measurement noise. The current trajectory of research reveals a convergence between model-driven and data-driven paradigms: while model-based approaches provide interpretability, data-driven techniques (ML and neural networks) offer adaptability and generalization capabilities. As projected by (El-Sheimy and Li, 2021), next-generation PLAN (Positioning, Localization, and Navigation) systems will be intelligent, self-learning, and dynamically adaptive-leveraging the synergistic integration of Artificial Intelligence (AI), Internet of Things (IoT), 5G communication, and edge computing technologies.

Methodology and System Design

The architecture of the proposed platform (Figure 1) was based on PDR as the core component of the navigation framework, responsible for the continuous tracking of user motion, while radio-based technologies served as the source of absolute positional corrections, essential for the periodic compensation of drift associated with IMU (Ali et al., 2021) (Kuang et al., 2024).

System Architecture Structure

The architecture of the platform was organized into four layers:

Data Acquisition Layer

The lowest layer of the architecture was responsible for direct interaction with hardware and the collection of raw sensor data. It enabled:

- Reading from the IMU,
- Scanning for BLE and UWB beacon signals.

The primary objective of this layer was to provide three synchronized data streams to higher layers. The first high-frequency and continuous data stream captured the user's motion dynamics. The second stream, from BLE beacons, provided periodic absolute positional references. RSSI values were incorporated into the measurement model of the EKF as inputs to a probabilistic radio propagation model, enabling position correction while accounting for high measurement uncertainty. The third stream was obtained from UWB beacons providing geometrically precise data.

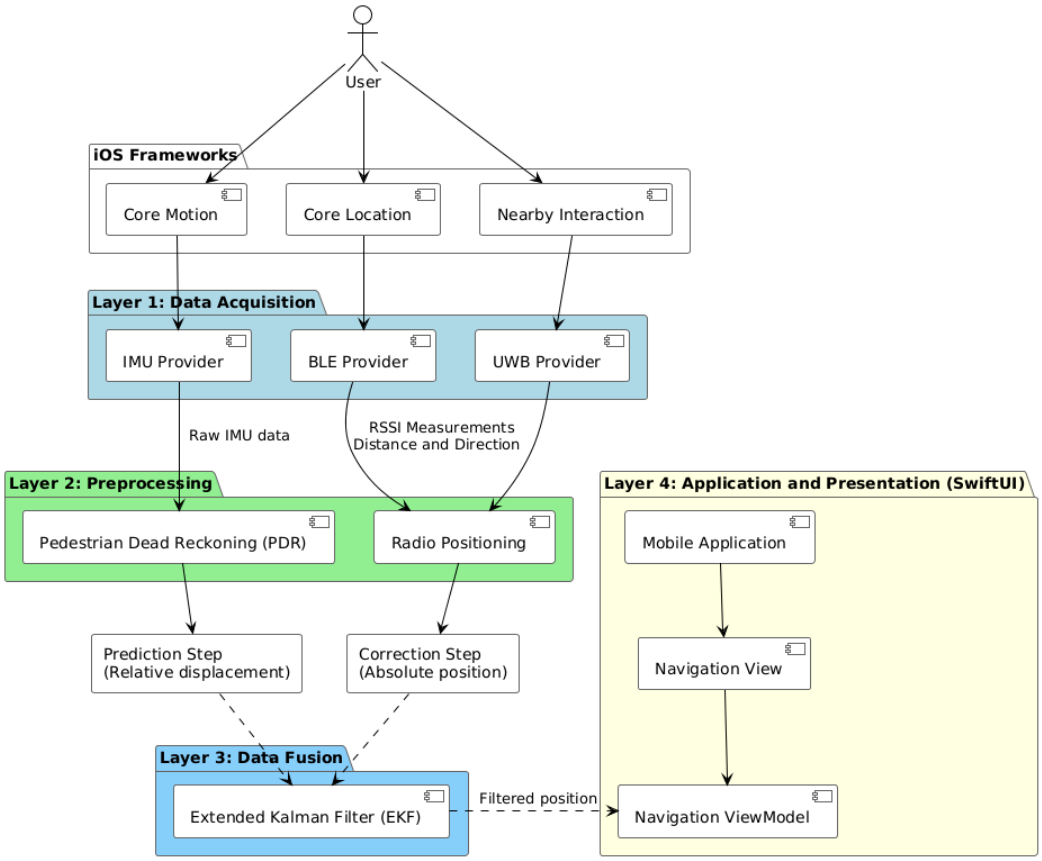

Fig 1. Diagram of the proposed platform architecture.

Preprocessing Layer

This layer was responsible for image evaluation hosting and allowed for the analysis of dermoscopic images using resource consuming algorithms. PerData from the acquisition layer was forwarded to preprocessing modules tasked with extracting features for the next stages:

- The PDR module processed IMU data to estimate the relative displacement of the user (step length and direction).
- The radio positioning module converted raw beacon data (BLE RSSI, UWB distance, and angle measurements) into absolute position estimates.

Data Fusion Layer

This layer was the logical core of the platform. The implemented EKF executed a cyclic prediction–correction process:

- Prediction utilized displacement data from the PDR module.
- Correction incorporated position estimates from the radio module (BLE or UWB) to mitigate accumulated drift errors, yielding a final filtered state estimate of the user's position and orientation.

Application and Presentation Layer

This layer managed user interaction, receiving the filtered position from the fusion layer and providing a visual representation. This layer was a:

- Research tool - enabling data recording and visualization for analytical purposes,
- Prototype navigation application - displaying the user's position on a map in real time

Interface and Visualization

Figure 2 illustrates the main interface of the research application. The central element was a dynamic 2D plot of the user's trajectory. The main portion of the screen is occupied by a dynamic 2D plot that visualizes the user's motion. Against the background of a grid and the marked positions of the UWB anchors (visible in the corners), key paths are rendered, such as the final EKF-derived trajectory (solid blue line), which represents the ultimate, filtered output of the sensor-fusion system, showing a smoothed and corrected estimate of the user's position. Another displayed element is the reference trajectory (dashed orange line), which serves as a benchmark for qualitative assessment.

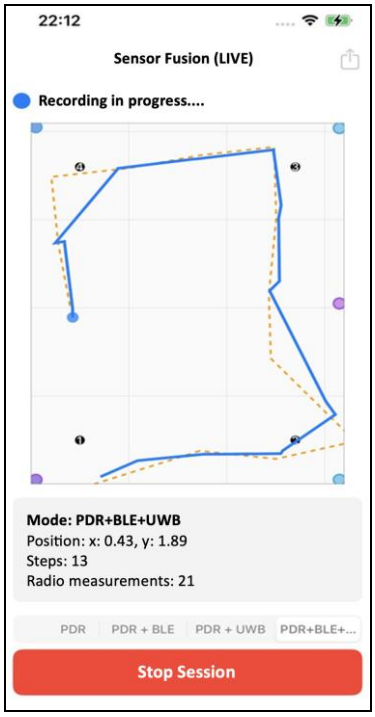

Fig 2. The visualization application used during the research.

The interface presented:

- the reference trajectory (ground truth),
- the PDR-derived trajectory (illustrating drift),
- position estimates from radio-based systems (BLE, UWB),
- the final filtered trajectory from the EKF.

This configuration enabled immediate qualitative assessment of the fusion process, allowing observation to which extent radio-based corrections mitigated PDR drift and how the EKF smoothed measurement noise from the radio systems.

The initial and fundamental step in configuring the filter was the definition of the state vector, i.e., the set of variables that the system estimated. The state vector had to comprehensively characterize the dynamics of the pedestrian, estimating not only position but also heading and velocity, which was crucial, as it enables more precise motion tracking and temporal propagation of uncertainty. The map functioned as a representation of the system state, with the user's estimated position serving as the primary state variable. Each new estimate provided by the EKF automatically updated the marker position (e.g., the blue dot) on the map.

Data Acquisition and Analysis

During the measurement session, all data was recorded with precise timestamps, encompassing:

- Raw sensor readings from IMU, BLE, and UWB,
- Outputs of the preprocessing modules (detected steps, position estimates),
- The final trajectory estimated by the EKF.

The data was stored in JSON format, facilitating subsequent analysis in external computational environments.

Experiment Configuration

Experiments were conducted in a room measuring approximately 3.2 × 4.1 m. The test environment included an active 2.4 GHz Wi-Fi access point, which could potentially interfere with RSSI measurements. Each trajectory was traversed at three distinct walking speeds to evaluate the impact of motion dynamics on the accuracy and stability:

- Slow: ~0.5 m/s
- Normal: ~1.0 m/s
- Fast: ~1.5 m/s

Test Scenarios

- PDR (IMU-only): Baseline data used to evaluate the drift magnitude inherent to the IMU.
- PDR + BLE: Fusion with corrections from BLE beacons, assessing the performance of a low-cost solution.
- PDR + UWB: Fusion leveraging UWB beacons, evaluating the accuracy of a commercial-grade UWB system.
- PDR + BLE + UWB: Hybrid system utilizing both correction sources to examine combined performance and robustness.

PDR Module and Kalman Filter Implementation

The Core Motion framework provides standardized access to the motion sensors of a mobile device. In addition to raw IMU readings, it enables access to processed pre-fused device motion data (Harle, 2013). Next, a peak detection algorithm is applied, registering a step when the signal amplitude exceeds a defined minimum threshold and a minimum time interval has elapsed since the previously detected step. This approach allows for the rejection of false detections and adaptation to the natural cadence of human walking. The prediction phase of the EKF is responsible for forecasting the system state at the next time step, relying solely on PDR-derived information. This step is executed at high frequency following each detected step. Step length is estimated using a nonlinear empirical model (Thrun, 2000), which correlates the user's motion dynamics with stride length. Step direction (heading) is derived from the device orientation quaternions converted to Euler angles, with the raw angle representing the forward direction.

During prediction, the filter also propagates state uncertainty, represented by the error covariance matrix. This is achieved through process model linearization using the Jacobian matrix and the incorporation of process noise. The process noise covariance matrix is a critical tuning parameter, reflecting uncertainty in the PDR model, including errors in stride length estimation and heading inaccuracies. Values were determined experimentally to realistically model IMU drift. The correction phase is triggered upon receiving new measurements from the radio positioning module (BLE or UWB). Its purpose is to correct the predicted state using these external absolute observations.

Measurement noise covariance is configured to differentiate filter confidence in BLE versus UWB data:

- UWB - low covariance, high correction weight, reflecting high precision.
- BLE - high covariance, low correction weight, preventing excessive positional fluctuations.

Additionally, an adaptive estimate weighting mechanism was implemented, enabling the automatic down-weighting of outlier measurements. Upon their detection, the system increases reliance on IMU-based predictions, which helps maintain stability and continuity of tracking even in the presence of disturbances.

Accuracy Assessment

The primary accuracy metric was defined as the RMSE, calculated as the square root of the mean of the squared differences between the estimated position and the reference (ground truth) position:

$$e_i = \sqrt{\left(x_{est,i} - x_{gt,i}\right)^2 + \left(y_{est,i} - y_{gt,i}\right)^2} \quad (1)$$

where ($x_{est,i}$, $y_{est,i}$) are the estimated coordinates, and ($x_{gt,I}$, $y_{gt,i}$) are the reference (ground truth) coordinates.
Then, for the entire trajectory consisting of Nmeasurement points, the RMSE was computed as follows:

$$RMSE = \sqrt{\frac{1}{N}\sum_{i=1}^{N} e_i^2} \quad (2)$$

The RMSE serves as a metric for both the precision and stability of the system, as it disproportionately penalizes large errors. Complementarily, the empirical Cumulative Distribution Function (CDF) of the localization error was employed, describing the proportion of errors not exceeding a specified threshold. The CDF analysis enables the determination of, among other metrics, the percentage of measurements achieving sub-meter accuracy and the system's operational stability across different configurations (PDR+BLE, PDR+UWB).

In addition to quantitative analysis, a qualitative evaluation of the trajectories was conducted, focusing on two aspects:

- Stability - the smoothness of the trajectory and absence of unnatural fluctuations.
- Continuity - the system's ability to maintain position estimates during temporary loss of radiometric signals.

High stability and continuity of trajectories indicate effective integration of the PDR module with the sensor fusion system and demonstrate the platform's resilience to environmental perturbations.

Results

The conducted study involved an experimental evaluation of the performance of the developed data fusion algorithm under laboratory conditions. Experiments were carried out for three walking-speed scenarios, representing different user dynamics. In each case, three variants of the fusion system were assessed:

- PDR+BLE - fusion of PDR with RSSI measurements from BLE beacons.
- PDR+UWB - integration of PDR with distance measurements based on UWB technology.
- PDR+BLE+UWB - a hybrid system combining both radiometric information sources.

PDR+BLE System

The Core Motion framework provides standardized access to the motion sensors of a mobile device. In addition to raw IMU readings, it enables access to processed pre-fused device motion data.

Slow walking (0.5 m/s)

The mean RMSE was 1.48 m, representing the highest error among all tested walking speeds. The empirical CDF analysis indicated that 50% of the measurements had an error below 1.41 m, while 90% of the measurements did not exceed 2.35 m.

Normal walking speed (1 m/s)

Figure 3 illustrates the comparison between the ground truth trajectory, the PDR trajectory, and the filtered fusion trajectory (PDR+BLE). Visual inspection demonstrates that the EKF effectively mitigates the drift introduced by PDR. However, due to the high variance of RSSI measurements, the fused trajectory (in blue) exhibits localized fluctuations, reflecting the limited stability of BLE-based corrections.

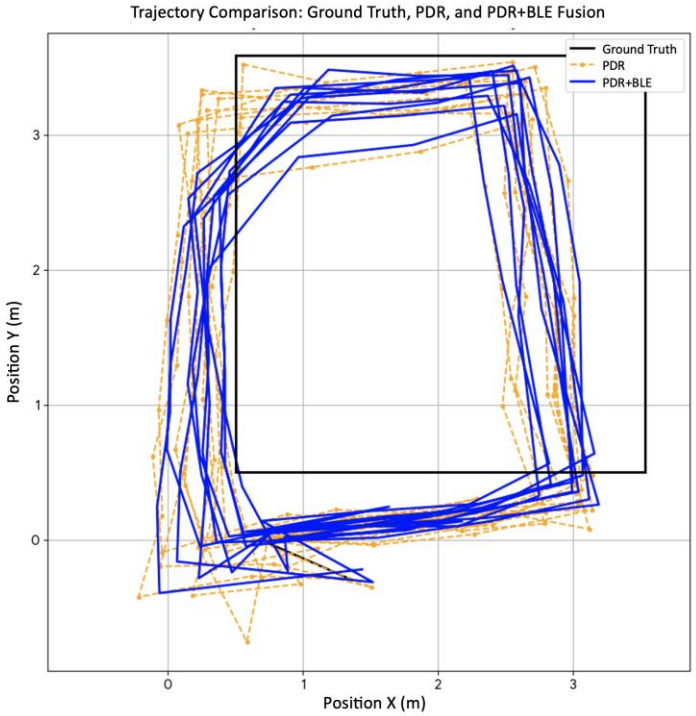

Fig 3. Comparison of PDR and PDR+BLE trajectories for normal walking speed.

The RMSE over 10 trials was 0.98 m, indicating a significant improvement compared to the standalone PDR system. The empirical cumulative distribution function (CDF) of the localization error (Figure 4) shows the median did not exceed 1.80 m, while 90% of the measurements exhibited an error below 3.51 m.

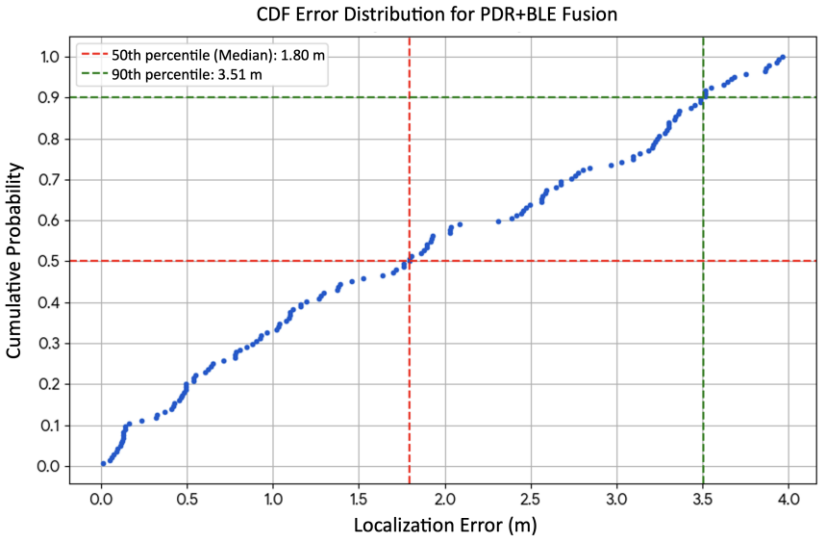

Fig 4. Empirical cumulative distribution function (CDF) of the localization error for the PDR+BLE system at normal walking speed.

Fast walking (1.5 m/s)

The RMSE reached 1.21 m. Comparison across all walking speeds indicated that the system achieved optimal accuracy at normal walking speed (RMSE = 0.98 m). Both slowing down and accelerating the gait resulted in degraded estimation quality. The increased error at slow walking can be attributed to the reduced precision of PDR and the longer accumulation time of orientation errors, whereas at fast walking, the shorter exposure time of the device to BLE beacon signals limited the number of available RSSI measurements.

PDR+UWB System

The second variant analysed relied on UWB technology, utilizing ToF measurements.

Slow walking (0.5 m/s)

Despite challenging conditions for PDR (the largest generated drift), the PDR+UWB fusion system demonstrated excellent performance, achieving an average RMSE of 0.24 m.

Normal walking speed (1 m/s)

Figure 5 illustrates the comparison between the PDR trajectory, PDR+UWB, and the reference path. The results show near-perfect alignment of the fused trajectory (green color) with the ground truth. Frequent and precise UWB corrections effectively eliminate PDR drift, resulting in a trajectory with high smoothness and stability.

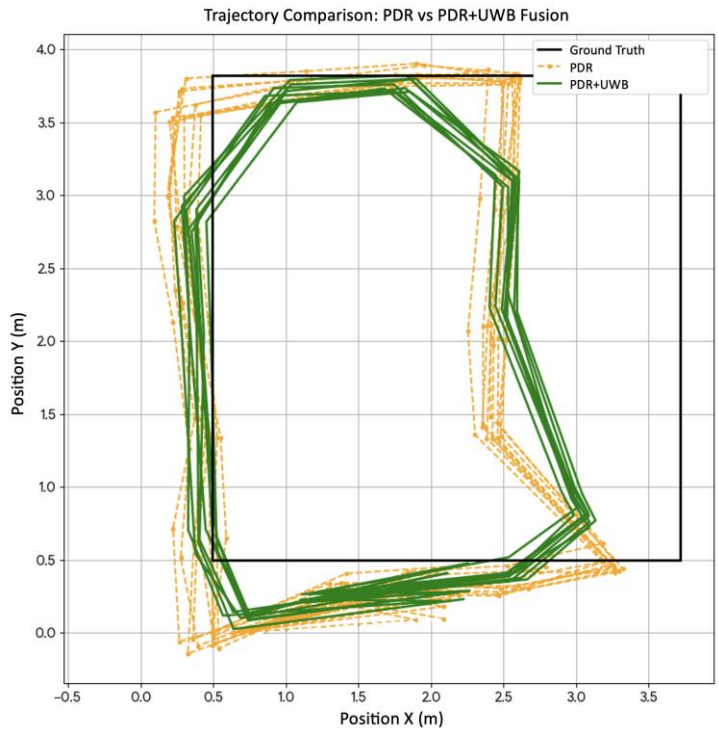

Fig 5. Comparison of PDR and PDR+UWB trajectories at normal walking speed.

The RMSE over 10 trials was 0.21 m, confirming the substantial superiority of UWB over BLE. From the empirical cumulative distribution function (Figure 6), it was observed that for 50% of the time, the localization error was less than 1.25 m, and for 90% of the measurements, it did not exceed 3.63 m.

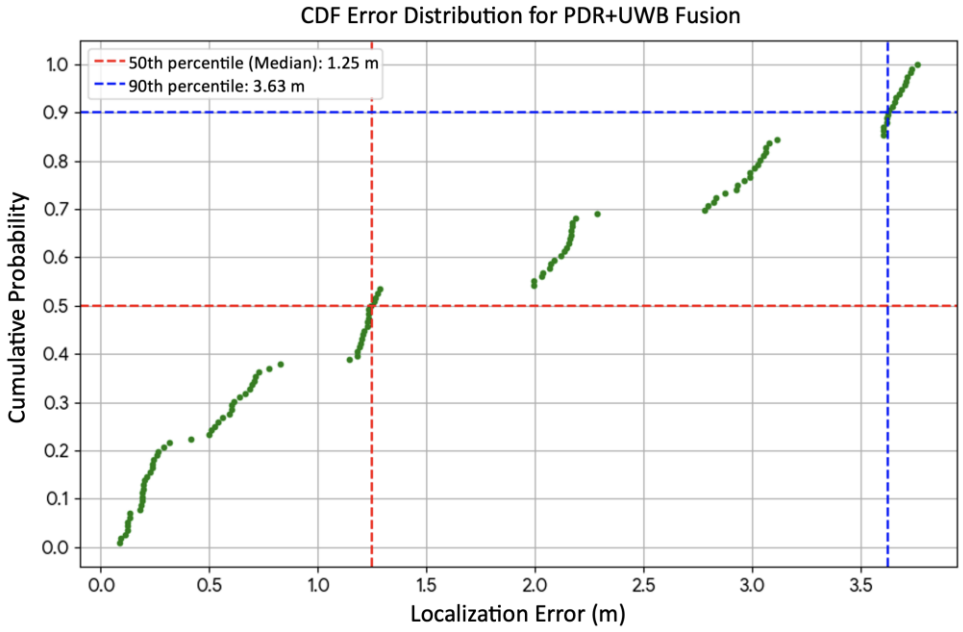

Fig 6. Empirical cumulative distribution function (CDF) of the localization error for the PDR+UWB system at normal walking speed.

Fast walking (1.5 m/s)

RMSE of 0.29 m was obtained. Comparative analysis indicates that the PDR+UWB system achieves the highest accuracy at normal walking speed (0.21 m). The system performed better under slow walking conditions (RMSE = 0.24 m) than fast walking. Although slow walking generates greater drift in autonomous PDR, the longer duration within the range of UWB anchors allows the Kalman Filter to collect more precise measurements and achieve more effective error correction. In all scenarios, the system maintains meter-level accuracy at the 90th percentile, confirming its high UWB reliability.

PDR+BLE+UWB System

The most comprehensive variant of the fusion system integrated data from PDR, BLE, and UWB. In this approach, the Kalman filter alternately utilized corrections from both radio systems, depending on signal availability. The analysis aimed to determine whether adding BLE measurements to the high-precision UWB system could further improve accuracy.

Slow walking (0.5 m/s)

The system achieved an RMSE of 0.23 m, representing a minimal improvement compared to the PDR+UWB variant.

Normal walking speed (1 m/s)

The best results were obtained at normal walking speed. Figure 7 presents a comparison of trajectories, while Figure 8 shows the error cumulative distribution. The RMSE was 0.20 m, representing the best result across all experiments. For 50% of measurements, the localization error did not exceed 1.41 m, and for 90% of measurements, it was below 3.45 m.

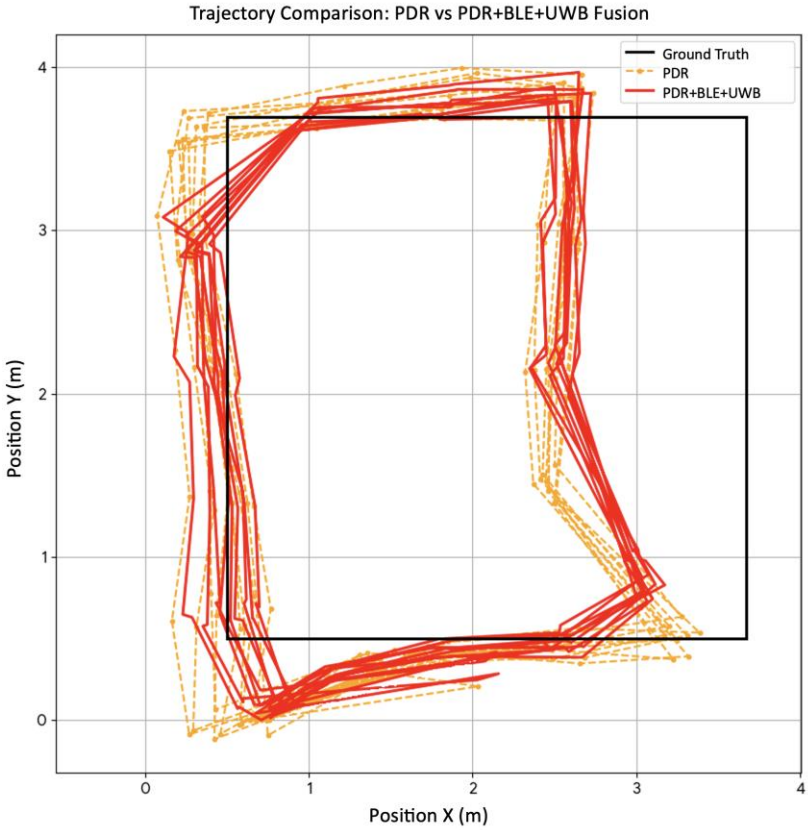

Fig 7. Comparison of PDR and PDR+BLE+UWB trajectories for normal walking speed.

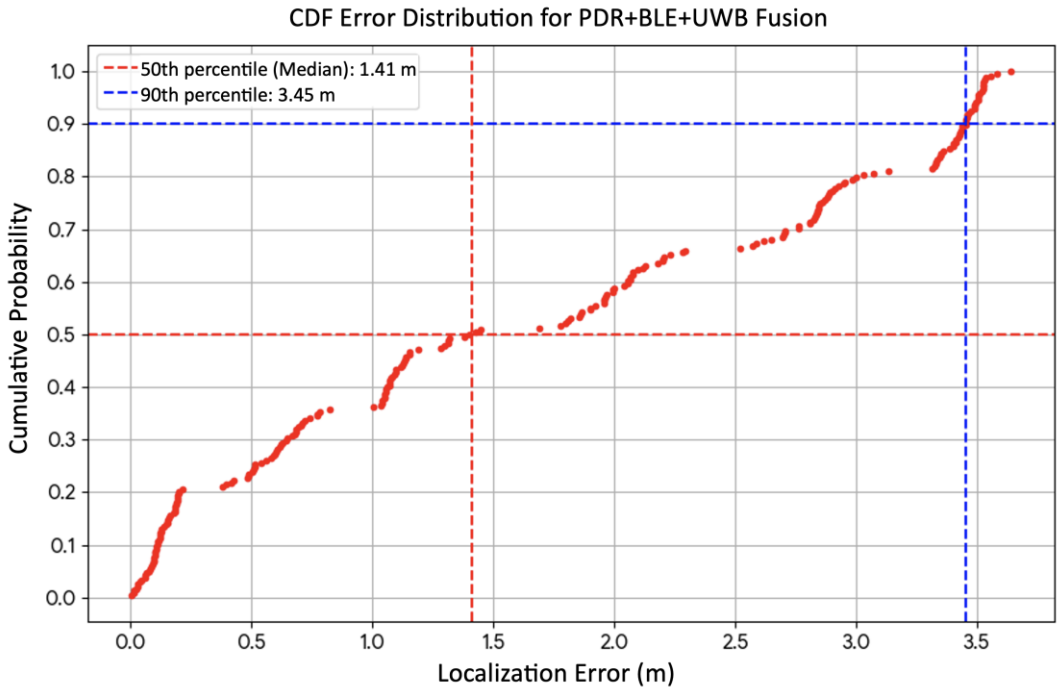

Fig 8. Empirical cumulative distribution function (CDF) of localization error for the PDR+BLE+UWB system at normal walking speed.

Fast walking (1.5 m/s)

An RMSE value of 0.28 m was obtained, which is comparable to that achieved in the PDR+UWB system.

Comparative analysis of fusion systems

A summary of the obtained error values is presented in Table 1. In all scenarios, the root mean square error remained at the decimetre level (ranging from 0.20 m to 0.28 m), providing conclusive evidence of the dominant role of UWB in the fusion process.

Table 1: Summary of the obtained error values for sensor fusion experiments.

Walking speed	PDR+BLE	PDR+UWB	PDR+BLE+UWB
Slow (0,5 m/s)	1.48 m	0.24 m	0.23 m
Normal (1 m/s)	0.98 m	0.21 m	0.20 m
Fast (1,5 m/s)	1.21 m	0.29 m	0.28 m

Both Figure 9 (comparison of the localization error CDF for all fusion systems) and Figure 10 (dependence of RMSE on walking speed) confirm that the fusion system integrating PDR and UWB is accurate and robust to variations in the user's walking dynamics.

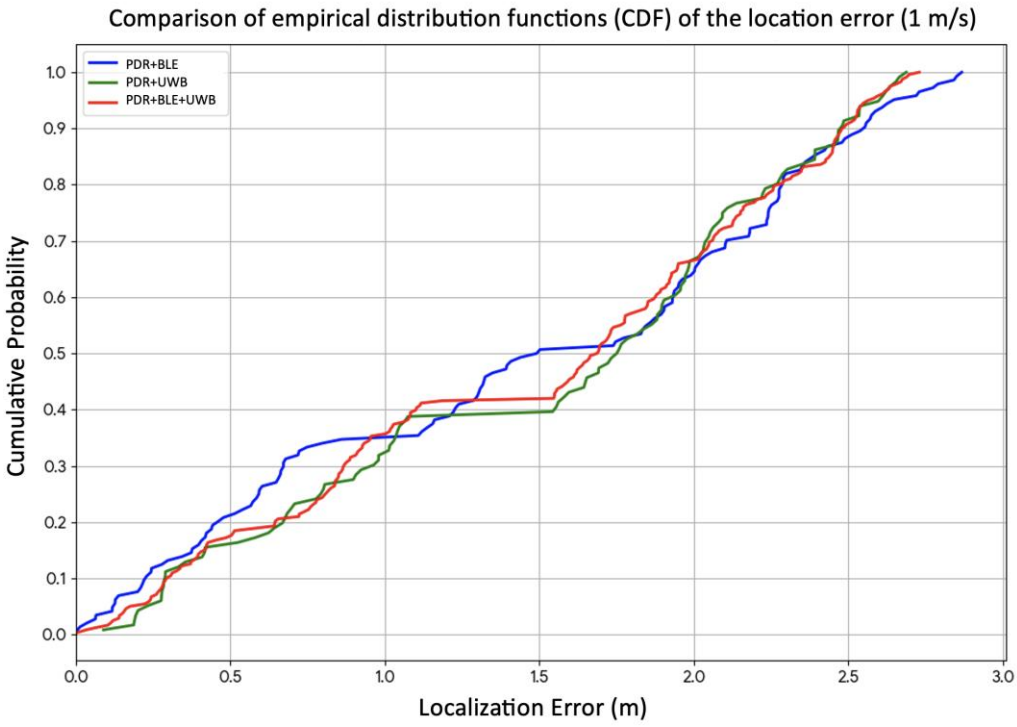

Fig 9. Comparison of localization error CDFs for normal walking speed.

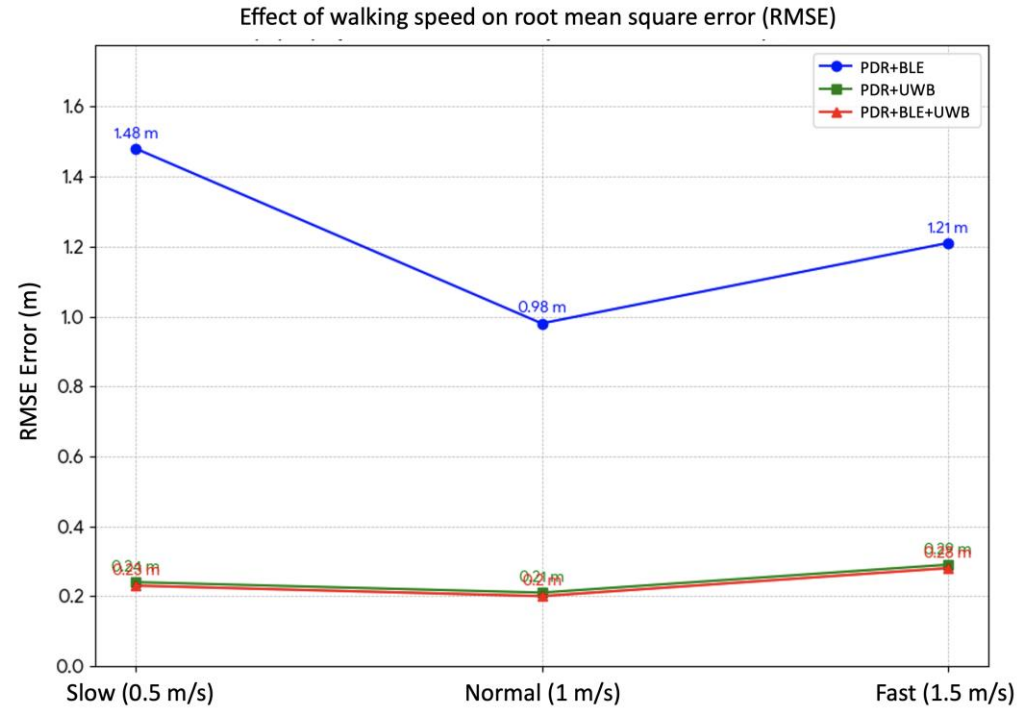

Fig 10. Influence of walking speed on the root mean square error (RMSE) of fusion systems.

Under optimal conditions (walking speed of 1 m/s), the PDR+UWB system (RMSE = 0.21 m) proved to be almost five times more accurate than the PDR+BLE system (RMSE = 0.98 m). This improvement results from the fact that

UWB, based on precise ToF measurements, provides much more stable data compared to the highly noisy RSSI-based measurements characteristic of BLE.

Conclusion

The conducted experimental studies aimed to evaluate the accuracy, stability, and continuity of the estimated trajectory across different system configurations.

For normal-speed walking, the Euclidean error between the estimated and actual endpoint ranged from 0.59 m to 1.45 m, with a mean error of 1.06 m, representing approximately 10% of the total traveled distance. For slow walking, errors ranged from 1.12 m to 2.25 m, with a mean endpoint error of 1.64 m. Faster walking (1.5 m/s) resulted in errors from 0.81 m to 1.55 m and a mean error of 1.15 m.

The results indicated that the autonomous PDR system is sensitive to the user's gait characteristics and cannot maintain high accuracy over extended periods, producing final errors of 10 - 15% of the traveled distance. The best performance was achieved at normal walking speed (1.06 m). Both slowing down (error increased up to 1.64 m) and speeding up (error increased up to 1.15 m) resulted in a loss of accuracy. Slow walking produced shorter steps, complicating their detection and length estimation, while the longer route duration caused gyroscope errors and orientation drift. Conversely, faster walking involved longer steps, which facilitated detection but led the empirical model to underestimate step length.

The results confirm that standalone PDR requires periodic position corrections and serves only as a supporting component in fusion-based systems, providing continuity of estimation between radio-based corrections. Data fusion with BLE and UWB systems significantly reduced errors accumulated by PDR. The PDR+BLE system achieved an RMSE of 0.98 m at normal walking speed, whereas PDR+UWB achieved 0.21 m, representing nearly a fivefold improvement in accuracy.

The PDR+BLE system exhibited substantial sensitivity to walking speed - RMSE increased to 1.48 m for slow walking and 1.21 m for fast walking. In contrast, UWB-based systems were significantly more resilient to changes in walking pace, maintaining decimeter-level accuracy. The highest error (RMSE = 0.29 m) occurred at fast walking due to fewer UWB corrections, while the best results (RMSE = 0.21 m) were obtained at 1 m/s.

User movement dynamics thus had a significant, yet differentiated, impact on system performance. All fusion systems achieved maximum accuracy at 1 m/s. BLE-based systems were the most sensitive to speed variations (RMSE range 0.98–1.48 m), whereas UWB systems maintained stable accuracy (0.20–0.29 m), demonstrating their robustness and predictability under realistic conditions.

In environments with good and continuous UWB signal coverage, adding BLE measurements did not provide significant improvement. The hybrid PDR+BLE+UWB system reached RMSE = 0.20 m at 1 m/s, almost identical to PDR+UWB (0.21 m). This phenomenon can be explained by the Kalman filter theory, in which the EKF dynamically weighs incoming data according to its uncertainty. UWB measurements are assigned low uncertainty, while noisy BLE data are automatically down-weighted by the Kalman gain, thus having minimal effect on the final state estimate.

Nonetheless, PDR fusion with BLE substantially improves accuracy compared to standalone PDR, providing precision sufficient for room-level navigation or zone determination. BLE, being a cheaper and simpler technology to deploy, remains useful in less demanding applications. In contrast, UWB allows sub-30 cm localization, outperforming BLE in terms of both precision and stability.

The comparison of PDR+UWB and PDR+BLE+UWB showed that adding BLE to a UWB-based system provides only marginal benefits, although a three-sensor architecture may be more reliable in large, complex environments where only UWB coverage is difficult or cost-prohibitive. In such cases, even imprecise BLE corrections can

mitigate PDR drift until coverage by at least three UWB anchors is regained, preventing system degradation and enhancing robustness.

In summary, the autonomous PDR system produced a mean error of 1.06 m (10% of the distance), fusion with BLE reduced it to 0.98 m, and fusion with UWB reduced it to 0.21 m. These results indicate that even occasional radio corrections effectively constrain IMU errors, while precise UWB corrections almost entirely eliminate drift. With regular and reliable UWB data, the EKF was able to reset accumulating uncertainty, maintaining estimation accuracy regardless of PDR prediction errors.
The results demonstrate that transitioning from single-sensor systems to fusion architectures represents a fundamental paradigm shift in indoor navigation design. It enables the creation of scalable, universal, and reliable solutions adapted to diverse environmental conditions. The choice of fusion strategy between the cheaper but less accurate BLE and the precise but costlier UWB should depend on the required level of accuracy and available resources.

A promising direction for further development is the use of artificial intelligence methods, such as recurrent neural networks (RNNs, especially Long Short-Term Memory - LSTM) or fuzzy logic systems. RNNs could be trained on accelerometer and gyroscope data from multiple users to learn gait patterns and estimate step length more accurately, dynamically adapting to individual movement styles. AI systems could also perform intelligent data weighting, analyzing signal quality from each sensor (e.g., UWB measurement variance, BLE stability) and dynamically deciding which data to trust. Such real-time EKF parameter tuning, e.g., decreasing the weight of disturbed UWB measurements and increasing reliance on PDR could significantly enhance the reliability and resilience of navigation systems under variable and unpredictable environmental conditions.

Acknowledgment

This research was funded by the project 07/010/BKM25/1052 at the Silesian University of Technology.

References

- Ahmad, N.S. (2024) “Recent Advances in WSN-Based Indoor Localization: A Systematic Review of Emerging Technologies, Methods, Challenges, and Trends,” IEEE Access, 12, pp. 180674–180714. Available at: https://doi.org/10.1109/ACCESS.2024.3509516.
- Ali, R. et al. (2021) “Tightly Coupling Fusion of UWB Ranging and IMU Pedestrian Dead Reckoning for Indoor Localization,” IEEE Access, 9, pp. 164206–164222. Available at: https://doi.org/10.1109/ACCESS.2021.3132645.
- Booranawong, A. et al. (2022) “Real-time tracking of a moving target in an indoor corridor of the hospital building using RSSI signals received from two reference nodes,” Medical and Biological Engineering and Computing, 60(2), pp. 439–458. Available at: https://doi.org/10.1007/S11517-021-02489-6/FIGURES/16.
- El-Sheimy, N. and Li, Y. (2021) “Indoor navigation: state of the art and future trends,” Satellite Navigation, 2(1). Available at: https://doi.org/10.1186/S43020-021-00041-3.
- Ferreira, A.F.G. et al. (2017) “Localization and Positioning Systems for Emergency Responders: A Survey,” IEEE Communications Surveys and Tutorials, 19(4), pp. 2836–2870. Available at: https://doi.org/10.1109/COMST.2017.2703620.
- Handbook of Multisensor Data Fusion: Theory and Practice, Second Editi (2025). Available at: https://www.routledge.com/Handbook-of-Multisensor-Data-Fusion-Theory-and-Practice-Second-Edition/LigginsII-Hall-Llinas/p/book/9781420053081 (Accessed: October 23, 2025).
- Harle, R. (2013) “A Survey of Indoor Inertial Positioning Systems for Pedestrians,” IEEE COMMUNICATIONS SURVEYS & TUTORIALS, 15(3). Available at: https://doi.org/10.1109/SURV.2012.121912.00075.
- Jiménez, A.R. et al. (2009) “A comparison of pedestrian dead-reckoning algorithms using a low-cost MEMS IMU,” WISP 2009 - 6th IEEE International Symposium on Intelligent Signal Processing - Proceedings, pp. 37–42. Available at: https://doi.org/10.1109/WISP.2009.5286542.

- Khodarahmi, M. and Maihami, V. (2023) “A Review on Kalman Filter Models,” Archives of Computational Methods in Engineering, 30(1), pp. 727–747. Available at: https://doi.org/10.1007/S11831-022-09815-7.
- Koutris, A. et al. (2022) “Deep Learning-Based Indoor Localization Using Multi-View BLE Signal,” Sensors 2022, Vol. 22, Page 2759, 22(7), p. 2759. Available at: https://doi.org/10.3390/S22072759.
- Kuang, Y. et al. (2024) “Tightly Coupled LIDAR/IMU/UWB Fusion via Resilient Factor Graph for Quadruped Robot Positioning,” Remote Sensing 2024, Vol. 16, Page 4171, 16(22), p. 4171. Available at: https://doi.org/10.3390/RS16224171.
- Lauzon, J.F. (2017) “Sensor Fusion and Deep Learning for Indoor Agent Localization Sensor Fusion and Deep Learning for Indoor Agent Localization Sensor Fusion and Deep Learning for Indoor Agent Localization.” Available at: https://scholarworks.rit.edu/theses (Accessed: October 23, 2025).
- Lin, Y. et al. (2024) “The State of the Art of Deep Learning-Based Wi-Fi Indoor Positioning: A Review,” IEEE Sensors Journal, 24(17), pp. 27076–27098. Available at: https://doi.org/10.1109/JSEN.2024.3432154.
- Mur-Artal, R., Montiel, J.M.M. and Tardos, J.D. (2015) “ORB-SLAM: A Versatile and Accurate Monocular SLAM System,” IEEE Transactions on Robotics, 31(5), pp. 1147–1163. Available at: https://doi.org/10.1109/TRO.2015.2463671.
- Poulose, A. and Han, D.S. (2019) “Hybrid Indoor Localization Using IMU Sensors and Smartphone Camera,” Sensors 2019, Vol. 19, Page 5084, 19(23), p. 5084. Available at: https://doi.org/10.3390/S19235084.
- Rosiak, M., Kawulok, M. and Maćkowski, M. (2024) “The effectiveness of UWB-based indoor positioning systems for the navigation of visually impaired individuals,” Applied Sciences-Basel, 14(13). Available at: https://doi.org/10.3390/APP14135646.
- Syazwani, N.C. et al. (2022) “Indoor Positioning System: A Review,” IJACSA) International Journal of Advanced Computer Science and Applications, 13(6), p. 2022. Available at: www.ijacsa.thesai.org (Accessed: October 23, 2025).
- Thrun, S. (2000) “Probabilistic Algorithms in Robotics,” AI Magazine, 21(4), pp. 93–93. Available at: https://doi.org/10.1609/AIMAG.V21I4.1534.
- UPPSATSER.SE: Design of a Method to Improve 5G Indoor Positioning Accuracy Using Sensor Fusion with an IMU and Floor Map Information (2025). Available at: https://www.uppsatser.se/uppsats/fd8a3c2e68/ (Accessed: October 23, 2025).
- Yapar, C. et al. (2023) “Real-Time Outdoor Localization Using Radio Maps: A Deep Learning Approach,” IEEE Transactions on Wireless Communications, 22(12), pp. 9703–9717. Available at: https://doi.org/10.1109/TWC.2023.3273202.
- Yeong, D.J. et al. (2021) “Sensor and Sensor Fusion Technology in Autonomous Vehicles: A Review,” Sensors 2021, Vol. 21, Page 2140, 21(6), p. 2140. Available at: https://doi.org/10.3390/S21062140.
- Yoon, P.K. et al. (2015) “Adaptive Kalman filter for indoor localization using Bluetooth Low Energy and inertial measurement unit,” Proceedings of the Annual International Conference of the IEEE Engineering in Medicine and Biology Society, EMBS, 2015-November, pp. 825–828. Available at: https://doi.org/10.1109/EMBC.2015.7318489.
- Zhang, F. et al. (2025) “Indoor Fusion Positioning Based on ‘IMU-Ultrasonic-UWB’ and Factor Graph Optimization Method.” Available at: http://arxiv.org/abs/2503.12726 (Accessed: October 23, 2025).